NO-Induced Reorganization of Porphyrin Arrays

Florian Buchner,[†] Knud Seufert,[‡] Willi Auwärter,[‡] Daniel Heim,[‡] Johannes V. Barth,[‡] Ken Flechtner,[†] J. Michael Gottfried,[†] Hans-Peter Steinrück,[†] and Hubertus Marbach[†,*]

[†]Lehrstuhl für Physikalische Chemie II and Interdisciplinary Center for Molecular Materials (ICMM), Universität Erlangen-Nürnberg, Egerlandstrasse 3, 91058 Erlangen, Germany, and [‡]Physik Department E20, Technische Universität München, James-Franck Strasse, 85748 Garching, Germany

ABSTRACT We studied the interaction of a highly ordered array of Co-tetraphenylporphyrin (CoTPP) with NO on Ag(111) by *in situ* scanning tunneling microscopy and X-ray photoelectron spectroscopy. Upon NO exposure, the initially quadratically ordered CoTPP layer reorganizes, showing a wealth of highly ordered NO+CoTPP coadsorbate phases with increasing size of the unit cell, interpreted as due to attractive lateral dipole−dipole interactions between the two species. The findings not only suggest a novel approach to control the arrangement of adsorbed porphyrins in particular but also should generally be considered in the production of functional layers from large organic molecules under ambient conditions or after exposure to small electronegative molecules.

The investigation of the self-assembly of large organic molecules has become a vividly explored, interdisciplinary field in science. One important goal is the tailored fabrication of highly ordered, molecular structures or networks, which are stabilized on a substrate, mostly a metal surface.[1−3] In this context, metalloporphyrins received particular attention[4−17] because they tend to form regular structures and their distinct intrinsic functionalities make them promising candidates for applications in chemical sensors,[18,19] solar cells,[20−22] and tailored catalytic processes.[23] The major tool for studying the molecular arrangement of such systems in the monolayer regime is scanning tunneling microscopy (STM).[4] Different factors were identified to determine the long-range order and the functional properties of molecular structures, in particular, the delicate balance between intermolecular and molecule−substrate interactions. Accordingly, specific molecular arrangements can be achieved by an appropriate choice of the corresponding ligands,[5−9] the substrate,[13] sample preparation,[8,24] and the usage of modified multicore porphyrin derivatives.[25]

One additional way to modify the properties of adsorbed layers of large organic molecules is the coadsorption of other organic molecules, which often leads to the formation of well-ordered mixed layers.[14,15,25−28] Interestingly, the influence of small coadsorbed molecules, such as CO or NO, on the arrangement of large organic molecules has not been addressed up to now, despite the fact that their intended or unintended (*e.g.*, in an ambient environment) coadsorption might lead to new ordered surface phases. Such effects are well-known for the small organic adsorbate

benzene on transition metal surfaces, such as Rh(111),[29] Ni(111),[30] or Ru(001).[31] The mutual stabilization of benzene and CO was employed in 1988 for imaging individual adsorbed benzene molecules for the first time in real space by STM.[32]

The interaction of small molecules such as NO, O_2, or CO with metalloporphyrin monolayers has been studied only under a quite different aspect, namely, their coordination to the central metal ion, a process that is of great interest due to the corresponding functionalities in biological systems. Recently, Flechtner *et al.* demonstrated in an XPS/UPS study that NO can be reversibly attached to Co-tetraphenylporphyrin (CoTPP) adsorbed on Ag(111) under ultrahigh vacuum (UHV) conditions.[33]

RESULTS AND DISCUSSION

In this work, we focus on a novel aspect of the interaction of NO with adsorbed CoTPP, namely, the lateral rearrangement of an initially quadratically ordered CoTPP layer upon exposure to NO. The rearrangement was monitored continuously *in situ* at room temperature (RT) and after individual
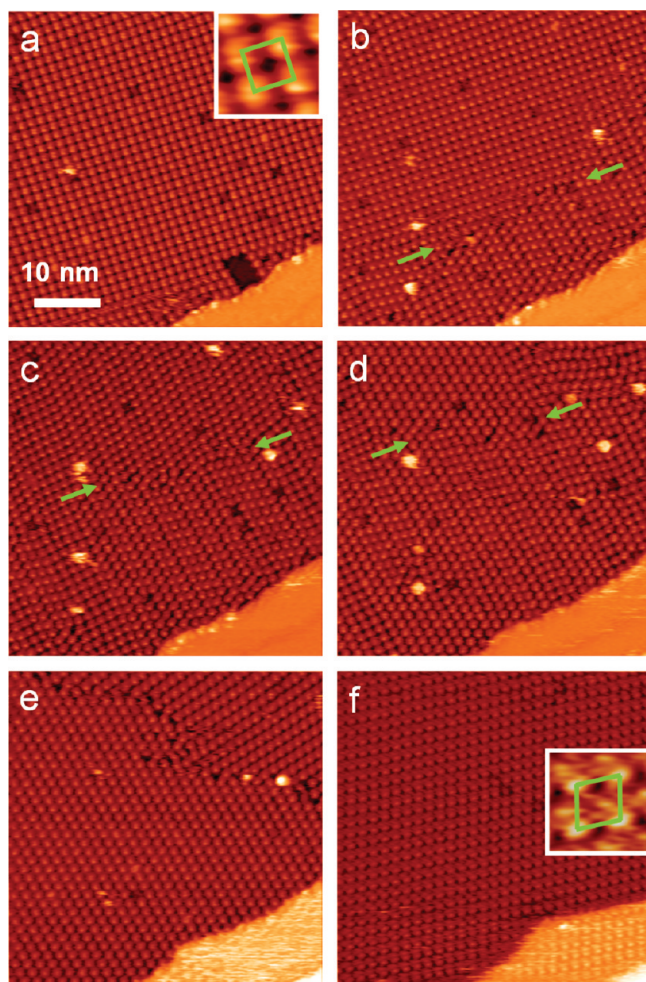
Figure 1. STM image series of a highly ordered array of CoTPP on Ag(111) during exposure to NO at RT. The corresponding NO dosages are (a) 576 L, (b) 606 L, (c) 640 L, (d) 677 L, (e) 755 L, and (f) 949 L. The rearrangement with increasing NO dose starting from the undisturbed square order in (a) to a hexagonal arrangement in (e) to an oblique structure in (f) is obvious and clearly develops toward larger unit cells. The unit cell areas as extracted from the experimental data are (a) 1.91 nm^2 and (f) 2.74 nm^2. All images have a size of 47 × 47 nm and were acquired at U_{BIAS} = −0.23 V and I_{SET} = 300 pA.

dosing steps also at low temperature (LT) by STM under UHV conditions, yielding an unprecedented number of different coadsorption phases. We present convincing evidence that this rearrangement process is induced by the coadsorption of NO and its incorporation in the porphyrin arrays.

Figure 1 shows a selection of STM images acquired at RT during exposure of an ordered CoTPP array (total coverage ~30% of monolayer saturation) on Ag(111) to NO gas (see Supporting Information for a movie file). Individual CoTPP molecules appear as protrusions.[34] Figure 1a was acquired at an NO dosage of 576 L (~2 h at 1×10^{-7} mbar). Up to this exposure, no significant changes in the CoTPP organization were observed. The square unit cell of CoTPP on Ag(111) with a lattice constant of ~1.4 nm is in agreement with previous studies of tetraphenylporphyrins on various substrates (see ref 4 and references therein).

In Figure 1b, which was acquired at 606 L (*i.e.*, 30 L after Figure 1a), the molecular order changed in the vicinity of the step edge and the dark rectangular area vanished and is now "filled" with CoTPP molecules. The boundary of the altered lateral arrangement is marked by the two arrows. After further exposure to NO, this boundary propagates away from the step edge, as indicated in Figure 1c,d. This proceeds until two domains with a slightly distorted hexagonal molecular arrangement are observed in Figure 1e. At even higher dosages of NO, the hexagonal structure continues to rearrange and finally transforms into the oblique structure without domain boundaries, as shown in Figure 1f. Analysis of the data reveals an increase of the unit cell area with increasing NO dosage, from initially 1.91 to 2.74 nm^2.

At this point, it should be noted that the axial coordination of NO to the central metal ion of CoTPP occurs already at much lower NO dosages.[33] This can indeed also be observed in our STM study (not shown here), but the molecules are easily removed upon scanning the sample at the tunneling conditions applied in the present work, leaving the molecular arrangement unchanged. We therefore conclude that NO coordinated to Co does not account for the observed rearrangement effects. This conclusion is also supported by the fact that a rearrangement upon NO exposure is also observed for the corresponding free base porphyrin layers (data not shown).

The most plausible explanation for the structural changes and the increasing size of the unit cell is the coadsorption of NO directly on the Ag(111) substrate. In this picture, the unit cell area increases as a result of the accumulation of NO coadsorbed between the CoTPP, that is, due to steric reasons. Note that there is a pronounced induction period corresponding to more than 500 L without changes in the initial square order, followed by continuous rearrangements (Figure 1b−f). This nonlinear process is interpreted as a delayed formation of a nucleus for the hexagonal phase as discussed in more detail below.

To obtain information on the azimuthal orientation and the intramolecular conformation within the CoTPP+NO layers, additional experiments with submolecular resolution were performed. A selection of images is shown in Figure 2 (all images = 6.95 nm × 5.35 nm), including scaled CoTPP models. The experiments were performed in two different experimental setups (LT-STM, RT-STM); they were measured after the denoted NO exposure in UHV either at 7 K (b−d) or 300 K (e,f). In Figure 2, the size of the unit cell of the CoTPP+NO structures increases continuously from 1.91 nm^2 (b) to 2.00 (c), 2.16 (d), 2.39 (e), and 3.16 nm^2 (f). Even though the shown superstructures have been obtained using different surface temperatures while dosing NO (c,d: 200 K; e,f: 300 K), overall CoTPP precoverages (c,d: ~30% of monolayer CoTPP; e,f: ~60%),
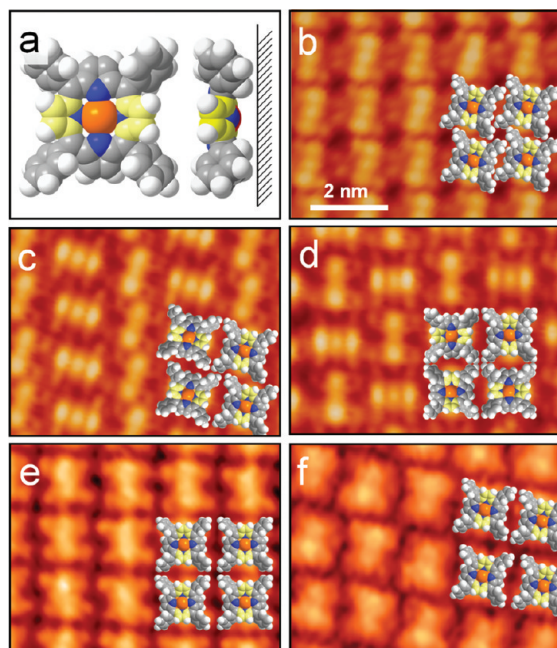
Figure 2. (a) Top and side view on space-filled models of CoTPP. The shown intramolecular conformation leads to a saddle shape appearance in STM due to the two pyrrole rings bent away from the surface (highlighted yellow). (b−f) STM images of ordered phases of CoTPP on Ag(111) before (b) and after (c−f) NO exposure at different temperatures (c,d: 200 K; e,f: RT). The corresponding values for NO exposure/temperature of measurement/tunneling parameters/ unit cell area are as follows: (b) 0 L/7 K/U_{BIAS} = −0.68 V, I_{SET} = 0.38 nA/1.91 nm^2; (c) 1000 L/7 K/U_{BIAS} = −0.77 V, I_{SET} = 0.12 nA/2.00 nm^2; (d) 1000 L/7 K/U_{BIAS} = −0.77 V, I_{SET} = 0.12 nA/2.16 nm^2; (e) 2368 L/RT/U_{BIAS} = −1.90 V, I_{SET} = 45 pA/ 2.39 nm^2; (f) 8399 L/RT/U_{BIAS} = −1.19 V, I_{SET} = 45 pA/3.16 nm^2.

and considering the discussed nonlinearity, it is clear that there is no simple relation between the size of the unit cell and a specific experimental parameter (*e.g.*, the expansion of the unit cell against NO dose differs from the data shown in Figure 1 compared to Figure 2); nevertheless, the size of the unit cell again generally expands with increasing NO dosage.

Figure 2b shows the STM image of the undisturbed CoTPP square arrangement, prior to NO exposure. A lengthy feature, denoted as main axis, dominates the appearance of an individual molecule and reflects the "saddle-shape" deformation of the adsorbed porphyrin macrocycle,[35] as shown in Figure 2a. In Figure 2c,d, two coexisting molecular arrangements imaged at 7 K after the exposure to 1000 L NO at 200 K are displayed. Even though the actually shown superstructures are coexisting in this experiment, it should be pointed out that the arrangement shown in Figure 2d was found to succeed the phase depicted in Figure 2c; that is, the latter was already observed after NO doses of 100 L. The analysis shows that not only the long-range order changes upon NO dosage but also the azimuthal orientation of the individual molecules. In Figure 2c, two out of four next neighbor CoTPP molecules have different orientation, whereas in Figure 2d, all four next

neighbors are rotated by 90°. Thus, the reorganization implies rotary motions and/or a change of the intramolecular conformation of CoTPP such that the main axis is rotated by 90°. This NO-induced rearrangement occurs already at 200 K; however, in a similar experiment at 160 K, no rearrangement was observed. In Figure 2e, an STM image acquired at RT after an exposure of 2368 L NO at RT is depicted. Now all molecules are arranged in a rectangular lattice with the main axes aligned along one of the unit cell vectors. Figure 2f shows the structure obtained for an NO dose of 8399 L at 300 K, with again a modified and expanded unit cell.

Inspection of the different images reveals that, despite the change in the lateral arrangement, the appearance and, thus, the intramolecular conformation of individual molecules in the different superstructures basically remain the same; this is immediately evident for Figure 2b−d at 7 K but also for Figure 2e,f at RT. It might be speculated that the minor deviations from the saddle-shape of individual CoTPP molecules in Figure 2f derive from accumulated coadsorbed NO or from a slight additional intramolecular deformation. In addition to the four ordered arrangements shown in Figure 2c−f, we found at least four other clearly distinguishable and partially coexisting CoTPP+NO phases (not shown here). In some cases, the rearrangement was completely reversible upon heating to ~500 K. Even though the experimental conditions (sample temperature during dosing, CoTPP precoverage) were not directly comparable, within one experimental run, always an expansion of the unit cell with increasing NO dosage was observed.

It should be noted that the basic findings presented so far were reproduced repeatedly in two different STM systems; however, some aspects such as the reversibility or the CoTPP coverage dependence will be further investigated.

Evidence for the coadsorption of NO is obtained from the data in Figure 3a, which shows a LT-STM image of CoTPP after exposure to 5000 L NO at RT. Upon close inspection of the micrograph, protrusions between the CoTPP molecules are discerned. These protrusions are associated with coadsorbed NO. Complementary spectroscopic information was acquired to verify this conclusion. Figure 3b shows an N 1s XP spectrum of a CoTPP monolayer after exposure to 6500 L NO at RT. Four components are identified, which are assigned to nitrogen atoms in the porphyrin macrocycle (purple), the NO molecule coordinated to Co in CoTPP (blue), the NO molecularly adsorbed on Ag(111) (red), and an unidentified species (green), in agreement with previous XPS studies of adsorbed NO/CoTPP complexes[33] and literature N 1s binding energies for NO on metal surfaces.[36] From the fact that the areas under the red (NO on Ag) and the purple (N in porphyrin) peak are very similar, one can conclude that roughly four NO molecules are coadsorbed per porphyrin. When the
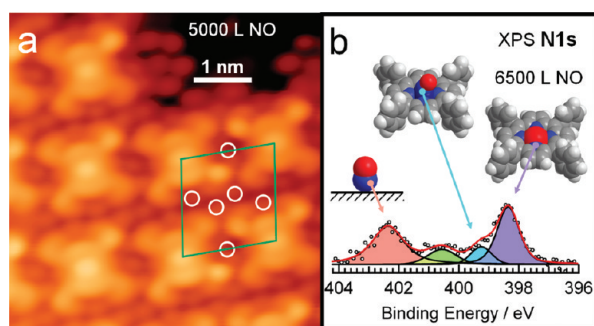
Figure 3. (a) STM image of CoTPP on Ag(111) acquired after 5000 L NO exposure at RT with $U_{BIAS} = -15$ mV, $I_{SET} = 50$ pA at 7 K, unit cell area = 2.79 nm². Between the porphyrins and on the presumably free Ag surface, small protrusions are visible, which are assigned to individual coadsorbed NO molecules (marked with white circles within the green unit cell). (b) N 1s region of the XP spectrum of a CoTPP layer on Ag(111) after exposure to 6500 L NO. The components of the N 1s signal are assigned to different nitrogen species as indicated.[33,36]

green peak was assigned to coadsorbed NO in a different local environment, this number would increase to approximately five NO molecules per CoTPP. Counting the protrusions in the STM image in Figure 3a within the unit cell yields a value of five protrusions per porphyrin, in good agreement with our interpretation. We therefore conclude that these protrusions are indeed due to individual NO molecules, evidencing the coadsorption of NO as the driving force for the observed rearrangement processes.

SUMMARY AND CONCLUSIONS

Considering the experimental evidence discussed above, we come to the following interpretation: The formation of well-ordered CoTPP+NO layers indicates that these coadsorbed structures are energetically favorable under the given experimental conditions. Initially, the undistorted CoTPP square arrangement does not provide adsorption sites for NO. Eventually, at a certain position, an adsorption site might emerge, for example, due to thermal movements of one or more porphyrin molecules, and an NO might adsorb at the corresponding site (note that the rearrangement was exclusively observed for NO dosage at sample temperatures above 160 K). This coadsorption then alters the positions of neighboring CoTPP molecules such that additional adsorption sites for NO emerge. Within this interpretation, a single coadsorption event (nucleus)

could trigger a chain of coadsorption processes, which can be observed in STM as a propagating reordering and results in the discussed nonlinearity of the rearrangement process.

Thus, upon NO coadsorption, the unit cell of the CoTPP arrays increases, indicating an increasing number of NO molecules per unit cell (note the filling of the hole in Figure 1a and the increasing appearance of molecules on the terrace in the lower right corner in Figures 1a–f). On the other hand, the interaction of NO with the bare Ag(111) surface is reported to be very weak, and no NO adsorption occurs on Ag(111) at RT for comparable or higher NO doses.[37,38] Nevertheless, when coadsorbed with CoTPP, NO is bound so strongly on the surface (stable up to ~450 K) that the energy cost of rearranging the CoTPP is overcompensated. We interpret this effect as due to significant attractive lateral dipole–dipole interactions of the electropositive CoTPP (which lowers the work function[39]) and the electronegative NO (which typically increases the work function[40]). These interactions can favor and stabilize a certain arrangement of the coadsorbates, for example, mixtures of two porphyrinoids with different electronegativity (NiTPP/F$_{16}$CoPc mixture), as demonstrated by Hipps et al.[14,15] Dipole–dipole interactions as well as substrate-mediated interactions were also suggested to stabilize mixed adlayers of the small hydrocarbon benzene with CO and NO on various transition metal surfaces, where CO and NO are strongly chemisorbed.[29–32,41] While we cannot rule out a contribution of substrate-mediated interactions for the system CoTPP+NO, they appear unlikely in view of the weak interaction of NO with the bare Ag(111) surface.

Regarding the richness of the observed structures in the presented system and the presumably general nature of the described process, one might envision the coadsorption of small molecules as an excellent tool to control the ordering, the intermolecular distances, and the molecule–substrate interactions of large functional molecules with high accuracy. In addition, similar effects have to be expected and considered quite generally in the production of functional layers from large organic molecules under ambient conditions or after exposure to small electronegative molecules.

METHODS

The experiments were performed in three separate (XPS, RT-STM, LT-STM) ultrahigh vacuum (UHV) systems with base pressures below 2×10^{-10} mbar. For the XPS measurements, a Scienta ESCA-200 spectrometer equipped with an Al Kα X-ray source (1486.6 eV), an X-ray monochromator, and a hemispherical energy analyzer (SES-200) was employed (for details, see refs 33 and 39). The RT-STM experiments were carried out using an RHK UHV VT STM 300 with RHK SPM 100 electronics (for details, see ref 34). The LT-STM data were recorded by a custom-

designed apparatus with a CreaTec STM (for details, see refs 9, 35, and 42 and references therein). All given voltages in STM refer to the sample, and the images were recorded in constant current mode. Moderate low pass filtering was applied for noise reduction. The STM data were processed with the software WSxM.[42]

Supporting Information Available: STM movie file in Quick-Time format, related information, and experimental details as a PDF file. This material is available free of charge *via* the Internet at http://pubs.acs.org.

REFERENCES AND NOTES

1. Barth, J. V. Molecular Architectonic on Metal Surfaces. *Annu. Rev. Phys. Chem.* **2007**, *58*, 375–407.
2. De Feyter, S.; De Schryver, F. C. Two-Dimensional Supramolecular Self-Assembly Probed by Scanning Tunneling Microscopy. *Chem. Soc. Rev.* **2003**, *32*, 139–150.
3. Barth, J. V.; Weckesser, J.; Cai, C. Z.; Gunter, P.; Burgi, L.; Jeandupeux, O.; Kern, K. Building Supramolecular Nanostructures at Surfaces by Hydrogen Bonding. *Angew. Chem., Int. Ed.* **2000**, *39*, 1230.
4. Gottfried, J. M.; Marbach, H. Surface-Confined Coordination Chemistry with Porphyrins and Phthalocyanines: Aspects of Formation, Electronic Structure, and Reactivity. *Z. Phys. Chem.* **2009**, *223*, 53–74.
5. Stöhr, M.; Wagner, T.; Gabriel, M.; Weyers, B.; Möller, R. Binary Molecular Layers of C_{60} and Copper Phthalocyanine on Au(111): Self-Organized Nanostructuring. *Adv. Funct. Mater.* **2001**, *11*, 175–178.
6. Spillmann, H.; Kiebele, A.; Stöhr, M.; Jung, T. A.; Bonifazi, D.; Cheng, F.; Diederich, F. A Two-Dimensional Porphyrin-Based Porous Network Featuring Communicating Cavities for the Templated Complexation of Fullerenes. *Adv. Mater.* **2006**, *18*, 275–279.
7. Veld, M. I.; Iavicoli, P.; Haq, S.; Amabilino, D. B.; Raval, R. Unique Intermolecular Reaction of Simple Porphyrins at a Metal Surface Gives Covalent Nanostructures. *Chem. Commun.* **2008**, *13*, 1536–1538.
8. Buchner, F.; Comanici, K.; Jux, N.; Steinrück, H.-P.; Marbach, H. Polymorphism of Porphyrin Molecules on Ag(111) and How to Weave a Rigid Monolayer. *J. Phys. Chem. C* **2007**, *111*, 13531–13538.
9. Auwärter, W.; Weber-Bargioni, A.; Riemann, A.; Schiffrin, A.; Groning, O.; Fasel, R.; Barth, J. V. Self-Assembly and Conformation of Tetrapyridyl-Porphyrin Molecules on Ag(111). *J. Chem. Phys.* **2006**, *124*.
10. Zhang, Z.; Imae, T. Hydrogen-Bonding Stabilized Self-Assembled Monolayer Film of a Functionalized Diacid, Protoporphyrin IX Zinc(II), onto a Gold Surface. *Nano Lett.* **2001**, *1*, 241–243.
11. Yokoyama, T.; Yokoyama, S.; Kamikado, T.; Okuno, Y.; Mashiko, S. Selective Assembly on a Surface of Supramolecular Aggregates with Controlled Size and Shape. *Nature* **2001**, *413*, 619–621.
12. Yanagi, H.; Mukai, H.; Ikuta, K.; Shibutani, T.; Kamikad, T.; Yokoyama, S.; Mashiko, S. Molecularly Resolved Dynamics for Two-Dimensional Nucleation of Supramolecular Assembly. *Nano Lett.* **2002**, *2*, 601–604.
13. Jung, T. A.; Schlittler, R. R.; Gimzewski, J. K. Conformational Identification of Individual Adsorbed Molecules with the STM. *Nature* **1997**, *386*, 696–698.
14. Hipps, K. W.; Scudiero, L.; Barlow, D. E.; Cooke, M. P. A Self-Organized 2-Dimensional Bifunctional Structure Formed by Supramolecular Design. *J. Am. Chem. Soc.* **2002**, *124*, 2126–2127.
15. Scudiero, L.; Hipps, K. W.; Barlow, D. E. A Self-Organized Two-Dimensional Bimolecular Structure. *J. Phys. Chem. B* **2003**, *107*, 2903–2909.
16. Scudiero, L.; Barlow, D. E.; Hipps, K. W. Physical Properties and Metal Ion Specific Scanning Tunneling Microscopy Images of Metal(II) Tetraphenylporphyrins Deposited from Vapor onto Gold(111). *J. Phys. Chem. B* **2000**, *104*, 11899–11905.
17. Scudiero, L.; Barlow, D. E.; Mazur, U.; Hipps, K. W. Scanning Tunneling Microscopy, Orbital-Mediated Tunneling Spectroscopy, and Ultraviolet Photoelectron Spectroscopy of Metal(II) Tetraphenylporphyrins Deposited from Vapor. *J. Am. Chem. Soc.* **2001**, *123*, 4073–4080.
18. Ashkenasy, G.; Ivanisevic, A.; Cohen, R.; Felder, C. E.; Cahen, D.; Ellis, A. B.; Shanzer, A. Assemblies of "Hinged" Iron-Porphyrins as Potential Oxygen Sensors. *J. Am. Chem. Soc.* **2000**, *122*, 1116–1122.
19. Santos, W. J. R.; Sousa, A. L.; Luz, R. C. S.; Damos, F. S.; Kubota, L. T.; Tanaka, A. A.; Tanaka, S. M. C. N. Amperometric Sensor for Nitrite Using a Glassy Carbon Electrode Modified with Alternating Layers of Iron(III) Tetra-(*N*-methyl-4-pyridyl)-porphyrin and Cobalt(II) Tetrasulfonated Phthalocyanine. *Talanta* **2006**, *70*, 588–594.
20. Hasobe, T.; Imahori, H.; Sato, T.; Ohkubo, K.; Fukuzumi, S. Enhancement of Light Harvesting and Photocurrent Generation by ITO Electrodes Modified with meso,meso-Linked Porphyrin Oligomers. *Nano Lett.* **2003**, *3*, 409–412.
21. Hecht, D. S.; Ramirez, R. J. A.; Briman, M.; Artukovic, E.; Chichak, K. S.; Stoddart, J. F.; Gruner, G. Bioinspired Detection of Light Using a Porphyrin-Sensitized Single-Wall Nanotube Field Effect Transistor. *Nano Lett.* **2006**, *6*, 2031–2036.
22. Imahori, H.; Fukuzumi, S. Porphyrin- and Fullerene-Based Molecular Photovoltaic Devices. *Adv. Funct. Mater.* **2004**, *14*, 525–536.
23. Benitez, I. O.; Bujoli, B.; Camus, L. J.; Lee, C. M.; Odobel, F.; Talham, D. R. Monolayers as Models for Supported Catalysts: Zirconium Phosphonate Films Containing Manganese(III) Porphyrins. *J. Am. Chem. Soc.* **2002**, *124*, 4363–4370.
24. Stadler, C.; Hansen, S.; Kroger, I.; Kumpf, C.; Umbach, E. Tuning Intermolecular Interaction in Long-Range-Ordered Submonolayer Organic Films. *Nat. Phys.* **2009**, *5*, 153–158.
25. Bonifazi, D.; Spillmann, H.; Kiebele, A.; de Wild, M.; Seiler, P.; Cheng, F. Y.; Güntherodt, H. J.; Jung, T.; Diederich, F. Supramolecular Patterned Surfaces Driven by Cooperative Assembly of C-60 and Porphyrins on Metal Substrates. *Angew. Chem., Int. Ed.* **2004**, *43*, 4759–4763.
26. de Wild, S. B. M.; Suzuki, H.; Yanagi, H.; Schlettwein, D.; Ivan, S.; Baratoff, A.; Güntherodt, H.-J.; Jung, T. A. A Novel Route To Molecular Self-Assembly: Self-Intermixed Monolayer Phases. *ChemPhysChem* **2002**, *3*, 881–885.
27. Yang, Z. Y.; Lei, S. B.; Gan, L. H.; Wan, L. J.; Wang, C.; Bai, C. L. The Effect of Polarity on Coadsorbed Molecular Nanostructures of Substituted Phthalocyanine and Thiol Molecules. *ChemPhysChem* **2005**, *6*, 65–70.
28. Wu, D. X.; Deng, K.; He, M.; Zeng, Q. D.; Wang, C. Coadsorption-Induced Reconstruction of Supramolecular Assembly Characteristics. *ChemPhysChem* **2007**, *8*, 1519–1523.
29. Mate, C. M.; Somorjai, G. A. Carbon Monoxide Induced Ordering of Benzene on Pt(111) and Rh(111) Crystal Surfaces. *Surf. Sci.* **1985**, *160*, 542–560.
30. Zebisch, P.; Huber, W.; Steinrück, H.-P. On the Formation of Mixed Ordered Structures in the Coadsorption System Benzene + NO on Ni(111). *Surf. Sci.* **1991**, *258*, 1.
31. Stichler, M.; Weimer, R.; Menzel, D. The Influence of Electronegative Coadsorbates on the Geometry of Benzene on Ru(001). *Surf. Sci.* **1997**, *384*, 179–191.
32. Ohtani, H.; Wilson, R. J.; Chiang, S.; Mate, C. M. Scanning Tunneling Microscopy Observations of Benzene Molecules on the Rh(111)-(3 × 3) (C_6H_6 + 2CO) Surface. *Phys. Rev. Lett.* **1988**, *60*, 2398–2401.
33. Flechtner, K.; Kretschmann, A.; Steinrück, H.-P.; Gottfried, J. M. NO-Induced Reversible Switching of the Electronic Interaction between a Porphyrin-Coordinated Cobalt Ion and a Silver Surface. *J. Am. Chem. Soc.* **2007**, *129*, 12110–12111.
34. Comanici, K.; Buchner, F.; Flechtner, K.; Lukasczyk, T.; Gottfried, J. M.; Steinruck, H. P.; Marbach, H. Understanding the Contrast Mechanism in Scanning Tunneling Microscopy (STM) Images of an Intermixed Tetraphenylporphyrin Layer on Ag(111). *Langmuir* **2008**, *24*, 1897–1901.
35. Weber-Bargioni, A.; Auwärter, W.; Klappenberger, F.; Reichert, J.; Lefrancois, S.; Strunskus, T.; Wöll, Ch.; Schiffrin,

A.; Pennec, Y.; Barth, J. V. Visualizing the Frontier Orbitals of a Conformationally Adapted Metalloporphyrin. *ChemPhysChem* **2008**, *9*, 89–94.

36. Pashutski, A.; Folman, M. Low Temperature XPS Studies of NO and N_2O Adsorption on Al(100). *Surf. Sci.* **1989**, *216*, 395.

37. Carley, A. F.; Davies, P. R.; Roberts, M. W.; Santra, A. K.; Thomas, K. K. Coadsorption of Carbon Monoxide and Nitric Oxide at Ag(111): Evidence for a CO−NO Surface Complex. *Surf. Sci.* **1998**, *406*, L587.

38. Zemlyanov, D.; Schlögl, R. Effect of Oxygen on NO Adsorption on the Ag(111) Surface: Evidence for a $NO_{3,ads}$ Species. *Surf. Sci.* **2000**, *470*, L20.

39. Lukasczyk, T.; Flechtner, K.; Merte, L. R.; Jux, N.; Maier, F.; Gottfried, J. M.; Steinrück, H. P. Interaction of Cobalt(II) Tetraarylporphyrins with a Ag(111) Surface Studied with Photoelectron Spectroscopy. *J. Phys. Chem. C* **2007**, *111*, 3090.

40. Bonzel, H. P.; Fischer, T. E. An UV Photoemission Study of NO and CO Adsorption on Pt(100) and Ru(101̄0) Surfaces. *Surf. Sci.* **1975**, *51*, 213.

41. Held, G.; Steinrück, H.-P. Cyclic Hydrocarbons. In *Landolt−Börnstein*; Bonzel, H. P., Ed.; Springer: Berlin, 2005; Vol. III/42, Subvol. A4, Chapter 3.8.7., pp 300−370.

42. Auwärter, W.; Schiffrin, A.; Weber-Bargioni, A.; Pennec, Y.; Riemann, A.; Barth, J. V. Molecular Nanoscience and Engineering on Surfaces. *Int. J. Nanotechnol.* **2008**, *5*, 1171–1193.

43. Horcas, I.; Fernandez, R.; Gomez-Rodriguez, J. M.; Colchero, J.; Gomez-Herrero, J.; Baro, A. M. WSXM: A Software for Scanning Probe Microscopy and a Tool for Nanotechnology. *Rev. Sci. Instrum.* **2007**, *78*, 013705.